

## Layer interaction in thin film CIS based photovoltaic device

*N.P.Klochko, N.D.Volkova<sup>\*</sup>, M.V.Dobrotvorskaya<sup>\*\*</sup>,  
P.V.Mateychenko<sup>\*\*</sup>, V.R.Kopach, V.I.Shkalet, S.N.Karasyov*

Kharkiv National Technical University "KhPI",  
21 Frunze St., 61002 Kharkiv, Ukraine

<sup>\*</sup>N.Zhukovsky National Aerospace University "KhAI",  
17 Chkalov Str., 61070 Kharkiv, Ukraine

<sup>\*\*</sup>Institute for Single Crystals, STC "Institute for Single Crystals",  
National Academy of Sciences of Ukraine,  
60 Lenin Ave., 61001 Kharkiv, Ukraine

*Received September 25, 2004*

The function of thin film photovoltaic device on the base of copper indium diselenide (CIS) depends immediately on the character of interactions in the layers being in contact therein: base CIS layer, buffer ZnSe layer, transparent conductive film of indium-tin oxide (ITO). Such interaction may occur during ZnSe electrodeposition from solution on the ITO or CIS surfaces as well as during vacuum annealing used in the technological process to modify the CIS crystal structure. The investigations using scanning electron microscopy, energy dispersing X-ray spectroscopy, electron-probe microanalysis, X-ray diffractometry, and X-ray photoelectron spectroscopy have shown that during vacuum annealing of the glass/Mo/CIS/ZnSe compositions, the buffer layer is purified of contamination, but the same annealing of the glass/Mo/ITO/ZnSe compositions enriches the buffer layer in indium and transforms it into  $ZnIn_xSe_y$ .

Функционирование тонкопленочного фотоэлектрического преобразователя (ФЭП) на базе диселенида меди и индия (CIS) непосредственно зависит от характера взаимодействия контактирующих в нем базового слоя CIS, буферного слоя ZnSe и прозрачной электропроводной пленки оксида индия и олова (ITO). Такое взаимодействие может иметь место как в процессе электрохимического осаждения ZnSe из раствора на поверхность ITO или CIS, так и в процессе вакуумных отжигов, используемых в технологическом процессе изготовления ФЭП для модификации кристаллической структуры CIS. Исследования методами электронной микроскопии в режимах сканирования поверхности и рентгеновского микроанализа, рентгеновской спектроскопии с дисперсией по энергиям, рентгеновской дифрактометрии и рентгеновской фотоэлектронной спектроскопии позволили обнаружить, что в процессе вакуумных отжигов композитов стекло/Mo/CIS/ZnSe буферный слой очищается от примесей, тогда как при отжигах композитов стекло/Mo/ITO/ZnSe он обогащается индием и превращается в  $ZnIn_xSe_y$ .

In [1], we have investigated composition and surface morphology of zinc selenide (ZnSe) films electrochemically deposited from solution and used as buffer layers in photovoltaic devices (PD) on the base of copper indium diselenide  $CuInSe_2$  (CIS). To simplify the investigation task, in the

above-mentioned work we have essentially excluded the interaction of zinc selenide with substrate by using chemically inert titanium nitride (TiN) substrate. Fulfilled X-ray photoelectron spectroscopy (XPS) and electron-probe microanalysis (EPMA) data considered in [1] show that during elec-

trodeposition, a film consisting of ZnSe and Zn(OH)<sub>2</sub> covered with Se<sup>0</sup>, SeO<sub>2</sub> and OSe(OH)<sub>2</sub> is formed at the TiN substrate surface. During vacuum annealing at 250–350°C, zinc hydroxide is transformed into zinc oxide, elemental selenium is partly desorbed and partly, along with Se<sup>4+</sup>, interacts with hydrogen occluded in the films and Zn(OH)<sub>2</sub> or ZnO forming ZnSe. So, vacuum annealing of zinc selenide films electrodeposited on TiN substrates at 350°C makes it possible to obtain ZnSe layers containing minimum impurities.

In real PV-devices, however, zinc selenide buffer layer is deposited not on the surface of inert material but on surface of CIS base layer or transparent conductive oxide, for example, on indium-tin oxide In<sub>2</sub>O<sub>3</sub>:Sn (ITO). As reported in [2], at increased temperatures (500°C) during PV-devices manufacture, an intense interaction of buffer ZnSe and base CuGaSe<sub>2</sub> (CGS) layers manifested itself as the Zn diffusion from ZnSe into CGS took place. Thus, to obtain the real information on composition of electrodeposited zinc selenide buffer layer in PV-device, it is necessary to take into account its interaction with contacting neighboring layers. Since the elaboration of high-efficiency thin film PV-devices on the base of CIS with ZnSe buffer layer is an actual task, the present work is devoted to investigation of such interaction before and after vacuum annealing.

The ZnSe films were electrodeposited from the electrolyte described in [1]. As substrates, glass sheets covered with magnetron sputtered transparent conductive oxides (ITO) were used as well as glass/Mo/CuInSe<sub>2</sub> compositions with magnetron sputtered molybdenum layers and 1–2 μm thick CuInSe<sub>2</sub> films electrodeposited and annealed in argon at 400°C in accordance with [3, 4]. Electrodeposition of zinc selenide was carried out in potentiostatic regime using a potentiostat provided with a programmer and electrochemical cell equipped with saturated Ag/AgCl reference electrode (SAE) ( $U_{SAE} = 0.22$  V vs. normal hydrogen electrode) and platinum counter electrode of 100 cm<sup>2</sup> area at cathode potential  $U_c = -1.15$  V vs. SAE. The electrolyte was agitated by a magnetic stirrer. During the electrolysis, the temperature was within limits of 30 to 40°C. Electrodeposition time was 2 to 20 min, the current density 0.5 to 2.0 mA/cm<sup>2</sup>. The thickness of so obtained zinc selenide layers, measured by means of Fizeau interferometer in accordance with [5]

increased with deposition time and current density from 0.02 μm to 0.16 μm. The as-electrodeposited ZnSe layers were annealed in vacuum (10<sup>-3</sup> Pa) at 250°C and 350°C during 0.5 h at each temperature. The surface morphology of CIS films and their bulk chemical composition were investigated by means of a scanning electron microscope LEO 1530 in the scanning (SEM) and energy dispersing X-ray spectroscopy (EDX) regimes. The film phase compositions were studied similar to [6] by XRD method using Philips PW 1820 goniometer with CuK<sub>α</sub>-radiation.

In addition, the sample surface morphology and composition were studied by electron-probe microanalysis (EPMA) using a JSM-820 electron microscope with a Link AN10/85S microanalysis system. The microscope resolution in this mode was 10 nm, the analyzed depth was about 1 μm. The composition of the sample ~10 nm thick sublayer was studied by X-ray photoelectron spectroscopy using a XPS-800 Kratos spectrometer. The sample surface compositions were determined using ratio of photoelectron spectra areas of C1s, O1s, Zn3p, Se3d, In3d, Cu3p, Mo3d core levels taking into account their sensitivity factors [7]. The binding energy ( $E_b$ ) was calibrated using C1s ( $E_b = 285$  eV) line as a reference. To determine the compounds present in the surface sublayers of the samples before and after the annealing, we analyzed the shapes of selenium, indium, copper, molybdenum and oxygen core-level spectra. For zinc, the shape of Auger electron spectra Zn<sub>LMM</sub> were considered because those are more sensitive to chemical state of the atom than Zn2p or Zn3p lines [8].

In order to appraise objectively the interaction between the buffer ZnSe and the base CIS layers, we have analyzed first of all the chemical composition and crystal structure of CIS layers electrodeposited from solution and annealed in argon flow at 400°C. Fig. 1 presents the EDX spectra of CuInSe<sub>2</sub> films characterized by stoichiometric metal content (Cu/In = 1.0) (Fig. 1a) and those containing excess indium (In/Cu = 1.4) (Fig. 1b). As is seen in Fig. 1, the EDX spectra for both samples contain, in addition to molybdenum substrate lines, copper, indium, selenium, and oxygen ones. According to [9], the oxygen peak in EDX spectra may evidence the existence of metal hydroxide impurities in such films. The XRD analysis of the base layers (Fig. 2) shows that stoichiometric CIS films and CIS films en-

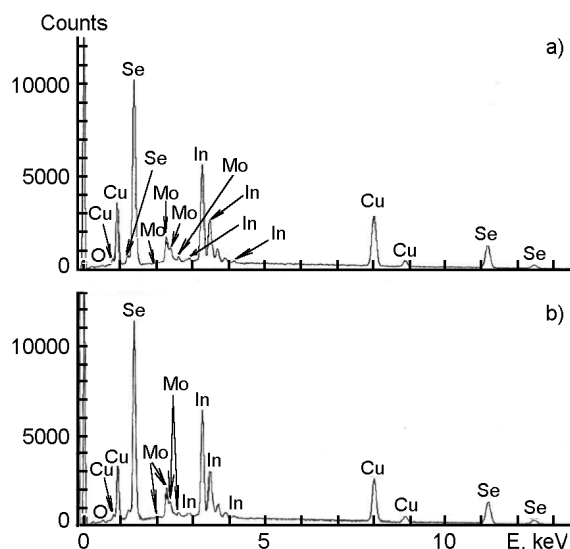


Fig. 1. EDX spectra of glass/Mo/CIS composites with CIS films: (a) stoichiometrical (25 at.% Cu, 26 at.% In, 49 at.% Se); (b) indium enriched (21 at.% Cu, 29 at.% In, 50 at.% Se).

riched in copper are single phased ones and exhibit the  $\text{CuInSe}_2$  (chalcopyrite) crystal structure (Fig. 2a, b). At the same time, the XRD pattern of indium-enriched CIS film (Fig. 2c) contains, along with this main phase, a small peak of  $\text{In}_2\text{Se}_3$  diffraction. In all X-ray diagrams, Mo and  $\text{MoSe}_2$  peaks are presented. Apparently, molybdenum selenide is an interaction product of molybdenum substrate and base layer during annealing of glass/Mo/ $\text{CuInSe}_2$  composite in argon flow at  $400^\circ\text{C}$ . As is seen in SEM pictures (Fig. 3), the copper-enriched CIS films are characterized by presence of crystal agglomerates up to  $2\ \mu\text{m}$  in diameter (Fig. 3a) while indium-enriched layers are nanocrystalline (Fig. 3b).

Investigations of glass/Mo/ $\text{CuInSe}_2$  composites using X-ray photoelectron spectroscopy have shown that  $\text{Se}3d$  XPS peaks are located at binding energy 54 eV, i.e. are characteristic for  $\text{Se}^{2-}$  in chemical compositions of copper, indium, and molybdenum selenides [7]. Both in indium-enriched CIS films and copper-enriched ones,  $\text{In}3d$  lines are located at energies of approximately 445 eV, that correspond to XPS spectra observed in [10] for CIS films. In thin surface sublayers ( $\sim 10\ \text{nm}$ ) of CIS films, adsorbed oxygen (line  $\text{O}1s$  at 532 eV) and oxygen bound with metals, for example in forms of  $\text{In}_2\text{O}_3$  or  $\text{Cu}_2\text{O}$  oxides (line  $\text{O}1s$  at 530 eV) is present. The surface composition of as-de-

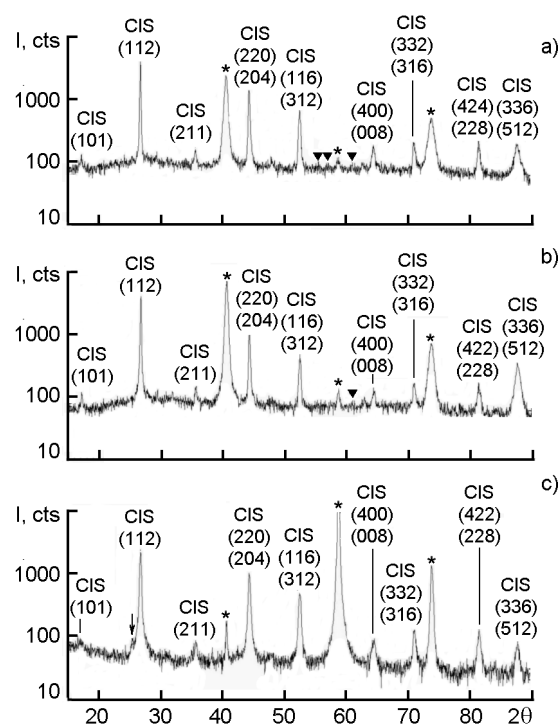


Fig. 2. XRD patterns of glass/Mo/CIS composites with CIS films annealed in flowing argon at  $400^\circ\text{C}$ : (a) copper enriched (28 at.% Cu, 23 at.% In, 49 at.% Se); (b) stoichiometrical (24 at.% Cu, 25 at.% In, 51 at.% Se); (c) indium enriched (21 at.% Cu, 29 at.% In, 50 at.% Se). The asterisks indicate Mo diffraction peaks; triangles,  $\text{MoSe}_2$  diffraction peaks; the arrow indicates the  $\text{In}_2\text{Se}_3$  diffraction peak.

posited glass/Mo/ $\text{CuInSe}_2$  sample and surface compositions of the samples obtained after deposition of zinc selenide onto this sample (glass/Mo/ $\text{CuInSe}_2/\text{ZnSe}$  samples N<sup>o</sup>1 and 2 prior to and after annealing) are presented in Table 1.

As a result of electrodeposition of zinc selenide buffer layers onto surfaces of copper-enriched, indium-enriched or stoichiometric CIS films, the indium and copper line intensities in XPS spectra decrease, but keep their positions, thus evidencing the undamaged structure and chemical composition of the base layer. Vacuum anneals at  $250^\circ\text{C}$  and  $350^\circ\text{C}$  do not result in shift of copper and indium peaks in the XPS spectra, but promote the changes in relative intensity of these peaks. Apparently, the decrease of Se and O contents resulting from vacuum annealing of glass/Mo/ $\text{CuInSe}_2/\text{ZnSe}$  composites can be considered as a consequence of water and

Table 1. Atomic concentrations of elements in the surface sublayers of the glass/Mo/CuInSe<sub>2</sub> and glass/Mo/CuInSe<sub>2</sub>/ZnSe composites according to XPS data

Sample	Composition, at.% ( $\pm 0.2$ %)						
	C	O	Se	In	Cu	Mo	Zn
glass/Mo/CuInSe <sub>2</sub>	44.0	26.6	6.1	12.9	9.4	1.0	–
glass/Mo/CuInSe <sub>2</sub> /ZnSe No.1	63.6	16.9	8.6	2.8	4.0	0.5	3.6
No.1 after vacuum annealing at 350°C	74.2	10.3	7.2	2.1	3.6	1.0	1.6
glass/Mo/CuInSe <sub>2</sub> /ZnSe No.2	53.2	19.4	9.8	0.8	1.0	0.7	14.5
No.2 after vacuum annealing at 350°C	56.8	16.2	8.9	2.7	3.4	1.0	10.0

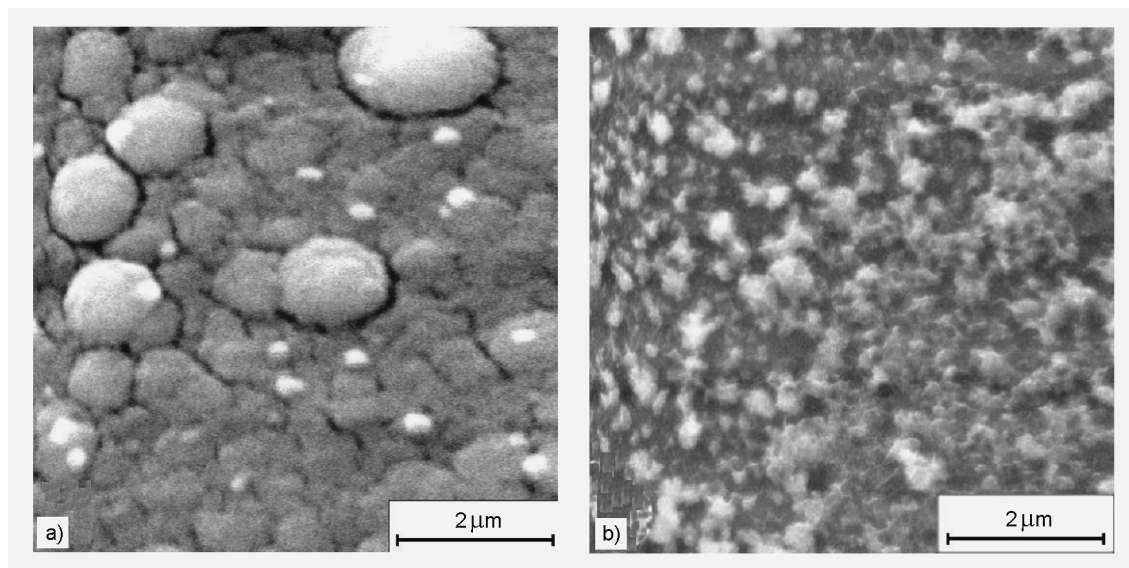
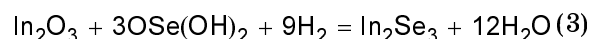
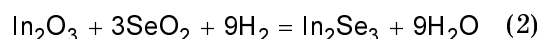
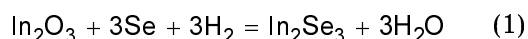


Fig. 3. Scanning electron micrographs of Ar-annealed at 400°C compositions glass/Mo/CIS with CIS films: (a) copper-enriched (28 at.% Cu, 23 at.% In, 49 at.% Se); (b) indium enriched (21 at.% Cu, 29 at.% In, 50 at.% Se).

excess selenium desorption that was observed during similar annealings of glass/TiN/ZnSe composites described in [1]. Moreover, during the annealings, we observed (Table 1) a decreasing Zn content that, in accordance with [10], may evidence recrystallizations of buffer layers as a result of Zn(OH)<sub>2</sub> into ZnO transformations and of diffusion of Zn into CIS by analogy with that described in [2]. As a whole, if the partial Zn diffusion into CIS is not taken into account, it can be concluded that buffer layer contacting with CIS is changed during vacuum annealing in the same way as it was changed in the case of contact with inert substrate TiN [1]: the zinc hydroxide and zinc oxide impurities interact with hydrogen and selenium occluded in the film in form of Se<sup>0</sup>, SeO<sub>2</sub>, or OSe(OH)<sub>2</sub> and so ZnSe is formed.

On the other side, in the case of electrodeposition of zinc selenide onto the ITO

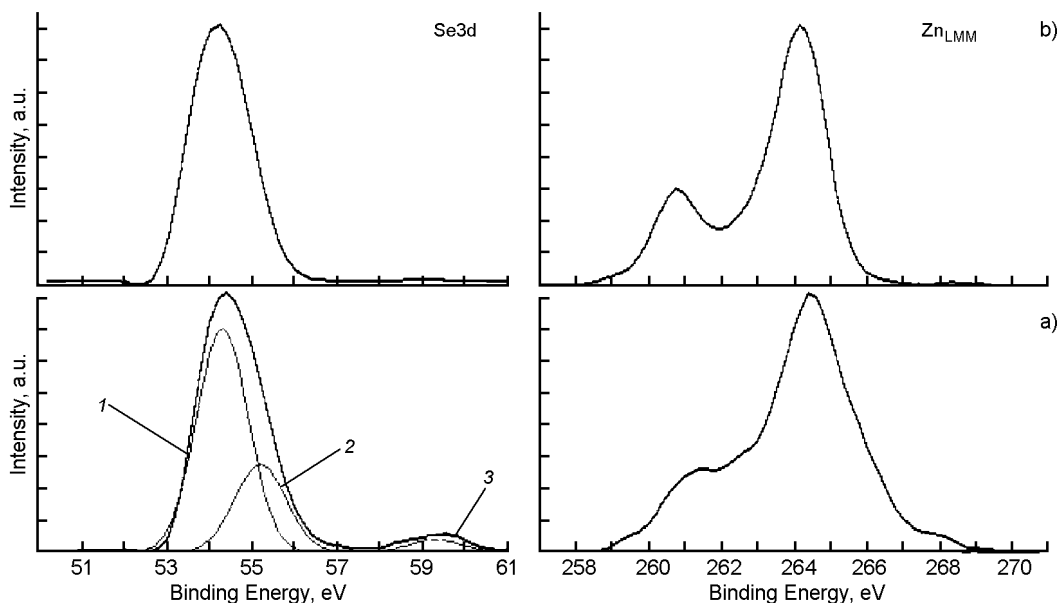
surface and of make-up of glass/ITO/ZnSe composite, the chemical interaction between buffer layer and substrate takes place during annealing at 250°C and 350°C, that is seen in XPS spectra as increasing intensities of In3d and Sn3d lines at binding energies corresponding to their selenides (Table 2). Perhaps the following reactions take place during vacuum annealings:



as well as similar reactions of tin oxides contained in ITO with hydrogen and selenium compounds, thus resulting in formation of tin selenides. Since the content ratio of indium to tin in ITO films is 9:1, it is reasonable to suppose that buffer layers on

Table 2. Atomic concentrations of elements in the surface sublayers of the glass/ITO/ZnSe composites according to XPS data

Sample	Composition, at.% ( $\pm 0.2\%$ )					
	C	O	Se	In	Sn	Zn
Sample No.3 glass/ITO/ZnSe	52.2	14.6	20.4	0.0	0.3	11.6
Sample No.3 glass/ITO/ZnSe after vacuum annealing at 250°C	43.9	21.7	8.7	6.3	1.5	17.9
Sample No.4 glass/ITO/ZnSe	59.3	9.0	25.6	0.5	0.1	5.5
Sample No.4 glass/ITO/ZnSe after vacuum annealing at 350°C	53.6	11.3	15.9	5.8	0.9	12.5

Fig. 4. XPS spectra of glass/Mo/CuInSe<sub>2</sub>/ZnSe sample No.1 before (a) and after (b) vacuum annealing at  $T = 350^\circ\text{C}$ .

ITO substrates after vacuum annealings consist of ZnSe and In<sub>2</sub>Se<sub>3</sub> with small impurities of tin selenides (Table 2). Note that In<sub>2</sub>Se<sub>3</sub> impurity in the buffer layer is not undesirable. In [11], this selenide itself is believed to be suitable as a buffer layer between CIS and transparent conductive oxide, while authors [12] point out the use of not only ZnSe or In<sub>x</sub>Se<sub>y</sub>, but also their compound ZnIn<sub>x</sub>Se<sub>y</sub>, as buffer layers to be of good promise. So, using zinc selenide electrodeposition on the ITO surface followed by vacuum annealing of glass/ITO/ZnSe composites, we can obtain a glass/ITO/ZnSe buffer layer being considered now as a prospective alternative for highly toxic cadmium-consisting buffer layer.

The interaction character of the buffer layer with CIS and ITO in glass/Mo/CuInSe<sub>2</sub>/ZnSe

and glass/ITO/ZnSe composites may be confirmed additionally by the changes in the Se3d and Zn<sub>LMM</sub> spectra shapes during the annealing (Fig. 4,5) similar to those observed in [1] for glass/TiN/ZnSe system. The Se3d core level spectra before annealing contain (Fig. 4a,5a) three components with binding energies of 54.2 eV (line 1), 55.3 eV (line 2), and 59.2 eV (line 3 in Fig. 4a), that can be ascribed to selenium in Se<sup>2-</sup> (ZnSe, In<sub>2</sub>Se<sub>3</sub>), Se<sup>0</sup>, and Se<sup>4+</sup> (SeO<sub>2</sub>, OSe(OH)<sub>2</sub>) states, respectively. After annealing, the spectra contain only a single line corresponding to Se<sup>2-</sup>.

In addition, the zinc selenide creation after annealing is confirmed by change in the Zn<sub>LMM</sub> Auger line shape. This line has a rather complex structure, so it is difficult to decompose it into components. However, the spectrum shape in Fig. 5b is typical for ZnSe [1, 8]. Note that prior to annealing

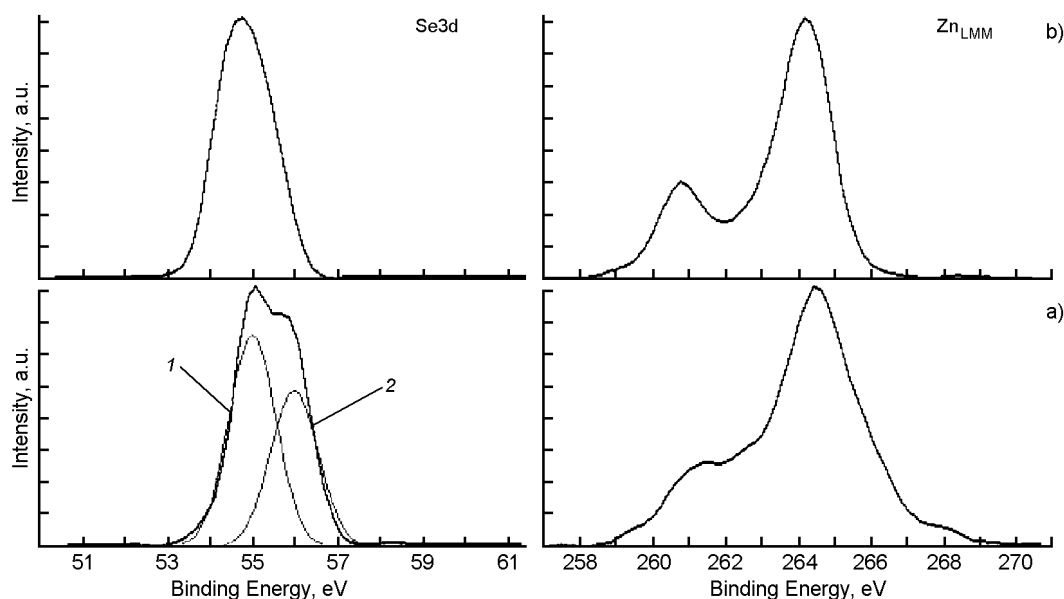


Fig. 5. XPS spectra of glass/ITO/ZnSe sample No.2 before (a) and after (b) vacuum annealing at  $T = 350^{\circ}\text{C}$ .

these spectra were mixed signals from ZnSe, ZnO,  $\text{Zn}(\text{OH})_2$ .

Thus, during the annealing of the glass/Mo/CuInSe<sub>2</sub> composite in argon flow at  $400^{\circ}\text{C}$ , the interaction of CIS base layer with molybdenum substrate resulting in formation of MoSe<sub>2</sub> takes place. In glass/Mo/CuInSe<sub>2</sub>/ZnSe composites, the partial diffusion of Zn from buffer layer into CIS, the removal of water and excess selenium out of the buffer layer, and transformation of zinc hydroxide and zinc oxide into ZnSe are observed during vacuum annealing at  $250^{\circ}\text{C}$  and  $350^{\circ}\text{C}$ . Alongside with the above, a partial interaction of ITO with selenium or their compounds and hydrogen occluded in the buffer layer takes place in glass/ITO/ZnSe composites under such vacuum annealing resulting in formation of indium selenides with small impurity of tin selenides. Thus, after the annealing, the buffer layer electrodeposited on ITO surface can be considered to be of  $\text{ZnIn}_x\text{Se}_y$  composition.

### References

1. N.P.Klochko, N.D.Volkova, M.V.Dobrotvorskaya et al., *Functional Materials*, **12**, 35 (2005).
2. S.Sadewasser, Th.Glatzel, M.Rusu et al., in: Proc. of 17th European Photovoltaic Solar Energy Conf., Munich, Germany (2001), p.1155.
3. N.P.Klochko, V.R.Kopach, A.A.Ryabchun et al., *Functional Materials*, **5**, 48 (1998).
4. N.P.Klochko, V.R.Kopach, V.O.Novikov et al., *Functional Materials*, **8**, 286 (2001).
5. Physics of Thin Films, ed. by G.Hass, R.E.Thun, Academic Press, New York (1969).
6. N.P.Klochko, V.R.Kopach, V.O.Novikov et al., *Functional Materials*, **7**, 843 (2000).
7. Practical Surface Analysis by Auger and X-ray Photoelectron Spectroscopy, ed. by D.Briggs, M.P.Seach, J.Wiley&Sons, New York (1983).
8. T.E.Gallon, in: Electron and Ion Spectroscopy of Solids, ed. by L.Fiermans, J.Vennik and W.Dekeyser, Plenum Press, New York, London (1978), p.236.
9. D.Johnston, K.M.Hynes, I.Forbes et al., in: Proc. of 17th European Photovoltaic Solar Energy Conf., Munich, Germany (2001), p.1082.
10. A.Ennaoui, C.D.Lokhande, M.Weber, in: Proc. of 14th European Photovoltaic Solar Energy Conf., Barselona, Spain (1997), p.1220.
11. G.Gordillo, C.Colderon, in: Proc. of 17th European Photovoltaic Solar Energy Conf., Munich, Germany (2001), p.1236.
12. M.Powalla, B.Dimmler, in: Proc. of 17th European Photovoltaic Solar Energy Conf., Munich, Germany (2001), p.983.

## **Взаємодія між шарами у тонкоплівковому фотоелектричному перетворювачі на базі CIS**

***Н.П.Клочко, Н.Д.Волкова, М.В.Добротворська,  
П.В.Матейченко, В.Р.Копач, В.І.Шкалето, С.М.Карасьов***

Функціонування тонкоплівкового фотоелектричного перетворювача (ФЕП) на базі диселеніду міді та індію (CIS) безпосередньо залежить від характеру взаємодії контактуючих у ньому базового шару CIS, буферного шару ZnSe та прозорої електропровідної плівки оксиду індію та олова (ITO). Така взаємодія можлива як протягом електрохімічного осадження ZnSe з розчину на поверхню ITO або CIS, так і під час вакуумних відпалів, які застосовуються у технологічному процесі виготовлення ФЕП з метою модифікації кристалічної структури CIS. Дослідження методами електронної мікроскопії у режимах сканування поверхні та рентгенівського мікроаналізу, рентгенівської спектроскопії з дисперсією за енергіями, рентгенівської дифрактометрії та рентгенівської фотоелектронної спектроскопії дозволили виявити, що під час вакуумних відпалів композитів скло/Mo/CIS/ZnSe буферний шар очищується від домішок, а внаслідок відпалів композитів скло/Mo/ITO/ZnSe він збагачується індієм і перетворюється у  $ZnIn_xSe_y$ .